ACS SENSORS

pubs.acs.org/acssensors Article

Mechanistic Approach for Long-Term Stability of a Polyethylene Glycol−Carbon Black Nanocomposite Sensor

Wenjun Li, Kazuki Nagashima,* Takuro Hosomi, Chen Wang, Yosuke Hanai, Atsuo Nakao, Atsushi Shunori, Jiangyang Liu, Guozhu Zhang, Tsunaki Takahashi, Wataru Tanaka, Masaki Kanai, and Takeshi Yanagida*

Cite This: *ACS Sens.* 2022, 7, 151−158 Read Online

ACCESS | Metrics & More | Article Recommendations | Supporting Information

ABSTRACT: Polymer−carbon nanocomposite sensor is a promising molecular sensing device for electronic nose (e-nose) due to its printability, variety of polymer materials, and low operation temperature; however, the lack of stability in an air environment has been an inevitable issue. Here, we demonstrate a design concept for realizing long-term stability in a polyethylene glycol (PEG)−carbon black (CB) nanocomposite sensor by understanding the underlying phenomena that cause sensor degradation. Comparison of the sensing properties and infrared spectroscopy on the same device revealed that the oxidation-induced consumption of PEG is a crucial factor for the sensor degradation. According to the mechanism, we introduced an antioxidizing agent (i.e., ascorbic acid) into the PEG−CB nanocomposite sensor to suppress the PEG oxidation and successfully demonstrated the long-term stability of sensing properties under an air environment for 30 days, which had been difficult in conventional polymer−carbon nanocomposite sensors.

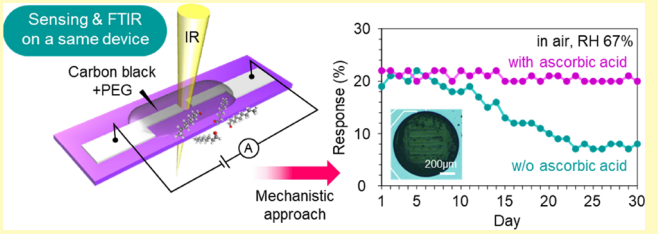

KEYWORDS: *chemiresistive sensor, carbon black, polyethylene glycol, nanocomposite, long-term stability*

Chemiresistive sensors, which transduce volatile molecules in surrounding environments into digital information, have recently gained increasing attention due to their ability to collect and monitor chemical information for various usages such as environmental monitoring, healthcare, food safety, and qualification of industrial fine products in upcoming Internet of Things (IoT) era.[1−8] Chemiresistive sensors are utilized as components of artificial olfaction system's so-called electronic nose (e-nose), and the molecular sensing data collected through the multisensor array in e-nose are analyzed based on a pattern recognition technique by mimicking the biological olfaction system.[9,10] The goal in this field is to collect time-series molecular sensing data by using IoT devices and exploit them as chemical big data.[11,12] Therefore, development of a long-term stable and low-energy consumption chemiresistive sensor is a major challenge. Among various chemiresistive sensors, a polymer−carbon nanocomposite-based sensor is a promising candidate for e-nose due to its printability, variety of applicable polymer materials, and low operation temperature (usually at room temperature),[13,14] which are hardly attainable in conventional metal-oxide semiconductor sensors.[15−21] Previous studies have been mainly devoted to polymer design for detecting various analyte molecules.[22−25] However, the polymer−carbon nanocomposite sensors often suffer from degradation of sensing performance in an air environment. For example, Chiou et al. reported that a polyethylene glycol/multiwalled carbon nanotube nanocomposite sensor exhibited degradation of sensing response to 46% of its initial value after 100 cycles of acetone sensing at 45 °C.[26] Wu et al. reported the degradation of the sensing response in a similar sensor device to ca. 50% of its initial value within 4 days at 25 °C in air.[27] These degradations of sensing responses strongly affect the pattern recognition performance in e-nose and plausibly cause fatal errors in data analysis. As such, a rational design concept to realize the long-term stable polymer−carbon composite sensor is strongly desired.

Here, we demonstrate a design concept for realizing long-term stability in a polyethylene glycol (PEG)−carbon black (CB) nanocomposite sensor under an air environment. Comparison of the sensing properties and infrared (IR) spectroscopy on the same device revealed that the oxidation-induced consumption of PEG is a crucial factor for sensor degradation. According to the mechanism, we introduced an antioxidizing agent (i.e., ascorbic acid) into the PEG−CB nanocomposite sensor to suppress the PEG oxidation and successfully demonstrate the long-term stability of sensing properties for 30 days, which had been

Received: September 2, 2021
Accepted: November 5, 2021
Published: November 17, 2021

https://doi.org/10.1021/acssensors.1c01875
ACS Sens. 2022, 7, 151−158

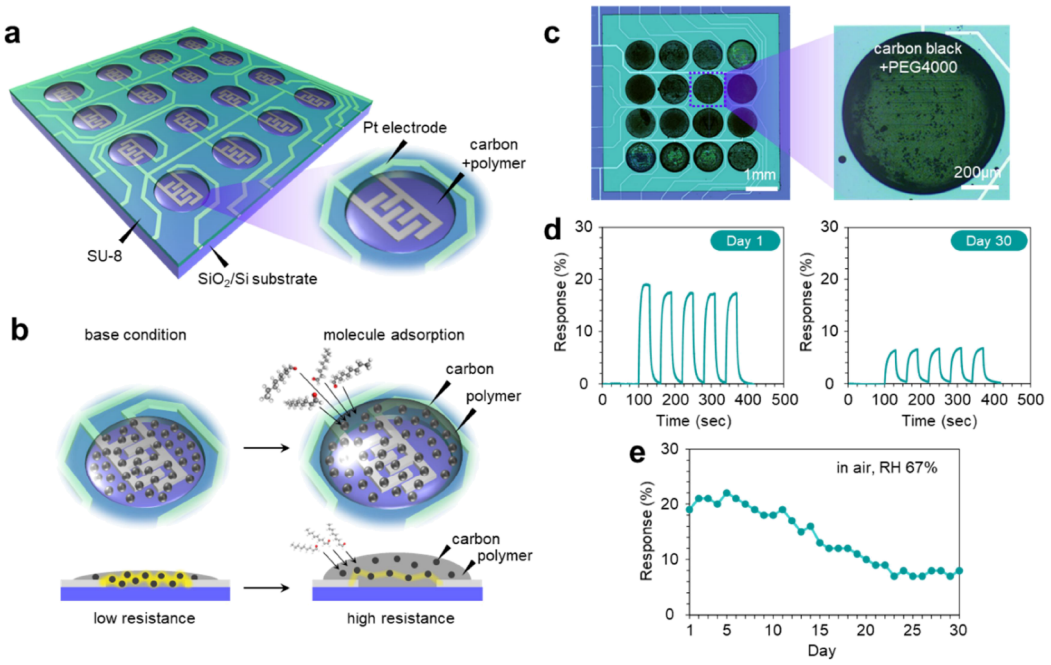

Figure 1. (a,b) Schematic illustrations of (a) chemiresistive sensor array and (b) the working principle of a polymer−carbon nanocomposite sensor. (c) Optical microscopy images of the chemiresistive sensor array (left) and a sensor device of PEG (PEG, PEG4000)−CB nanocomposite (right). (d) Successive sensing responses to 2.7 ppm nonanal at Day 1 (left) and Day 30 (right). (e) Duration of the sensing response to 2.7 ppm nonanal when storing the sensor sample at room temperature in air with RH 67%. All sensing measurements were performed at room temperature in air with N_2 carrier gas.

difficult in conventional polymer−carbon nanocomposite sensors.

RESULTS AND DISCUSSION

Figure 1(a,b) shows the schematic images of the polymer−carbon nanocomposite-based chemiresistive sensor array and its working principle. The sensor consists of electrically conductive carbon nanoparticles and an electrically insulative polymer. In previous studies, 16 types of gas chromatography stationary phases, which exhibit a wide range of adsorption properties for volatile molecules, were selected as polymer materials for e-nose.[28,29] The adsorption of analyte molecules in the polymer matrix induces a volumetric change of the nanocomposite, leading to the increase of electrical resistance by extending the distance between the carbon nanoparticles. Figure 1c shows the optical microscopy images of the polymer−carbon nanocomposite-based chemiresistive sensor array and a sensor device composed of a PEG−CB nanocomposite (PEG 4000, m.w. 3600−4400). PEG is a typical polymer material for the polymer−carbon nanocomposite sensor,[30,31] which enables the detection of a variety of polar molecules. The PEG−CB nanocomposite has a granular shape as shown in the Supporting Information Figure S1. Figure 1d shows the successive sensing responses of a PEG−CB nanocomposite sensor to 2.7 ppm nonanal at Day 1 and Day 30. Nonanal is a component of perfume,[32] an attractant for *Culex* mosquitoes,[33] an indicator for lipid peroxidation in muscle foods,[34] and a lung cancer biomarker in exhaled breath.[35] The sensing measurements were conducted once a day at room temperature in air with flowing N_2 carrier gas, and at other times, the device was stored at room temperature in air with 67% relative humidity (RH) under dark conditions. The sensing response significantly decreased to ca. 30% of its initial value within 30 days, which is consistent with the previous studies.[36,37] Such a decreasing tendency of the sensing response is more clearly seen in Figure 1e. During the test, the device experienced 150 cycles of molecular sensing. Since the stable sensing response was still observed even after the successive 150 cycles of molecular sensing at Day 1 (Figure S2), the degradation of the sensing response must originate from storing the device rather than from the molecular sensing operation. Thus, the degradation of the sensing response under an air environment is proven to be an inevitable issue in a PEG−CB nanocomposite sensor.

In order to specify what caused the degradation of the sensing response, we designed a PEG−CB nanocomposite sensor device capable of performing both molecular sensing and IR spectroscopy on the same device by precisely controlling the gap size of Pt electrodes and the thickness of the nanocomposite (see details in the Experimental Section). Such a "2-way device" allows us to directly link the variations of molecular sensing properties and chemical states of the nanocomposite sensor. Figure 2a,b shows the schematic illustration and the photo of the 2-way device, respectively. By using the 2-way device, we first conducted molecular sensing with aging tests under various environments. Figure 2c shows the sensing responses of the 2-way device to 2.7 ppm nonanal at Day 1 and Day 6 for the aging tests in air with RH 0%, N_2 with RH 95%, and N_2 with RH 0%. The aging tests were conducted at 120 °C. Significant degradations of the sensing response were observed at Day 6 in air with RH 0% and N_2 with RH 95%, while the sensing response in N_2 with RH 0% was almost unchanged. Under the former two conditions, the degradation started from Day 2 and progressed with increasing time as shown in Figure 2d. The aging test in O_2 with RH 0% revealed that the observed degradation in air with RH 0% was crucially governed by oxygen (Figure S3). These results suggest that both oxygen and water are the major factors for the degradation of the sensing response

https://doi.org/10.1021/acssensors.1c01875
ACS Sens. 2022, 7, 151−158

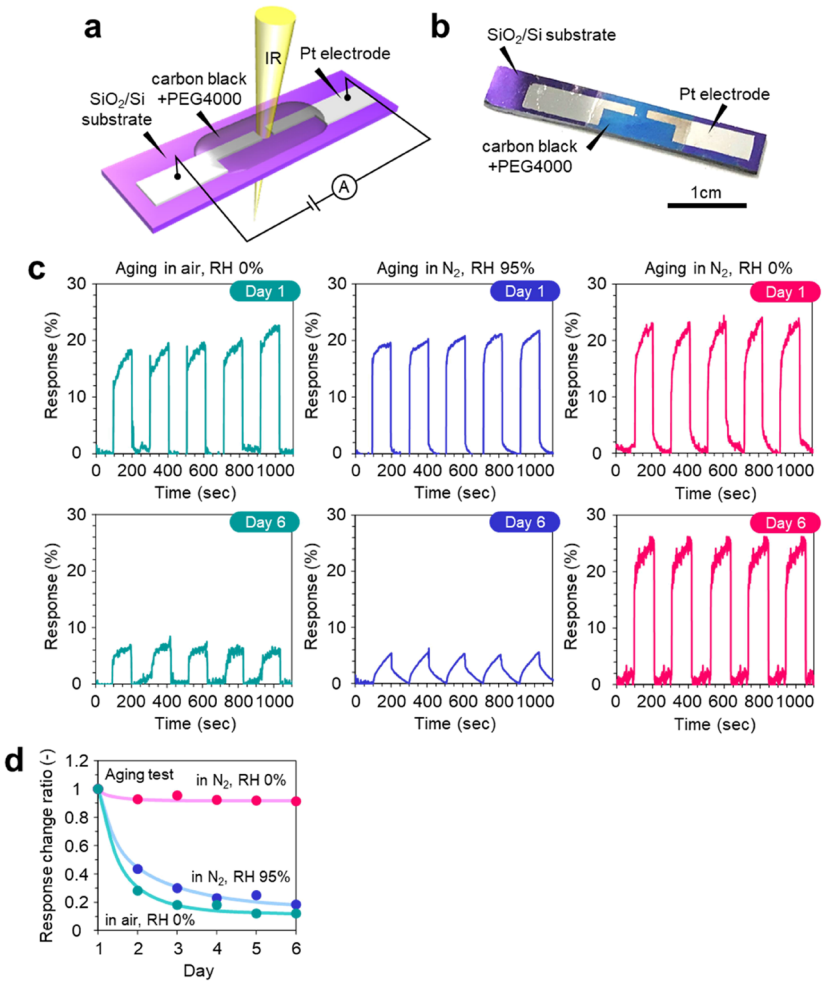

Figure 2. (a) Schematic illustration and (b) photo of the 2-way device capable of performing molecular sensing and IR spectroscopy on the same device. (c) Successive sensing responses to 2.7 ppm nonanal at Day 1 (upper) and Day 6 (lower) when aging the devices in air with RH 0% (left column), N_2 with RH 95% (middle column), and N_2 with RH 0% (right column), respectively. (d) Duration of the sensing response (i.e., response change ratio) to 2.7 ppm nonanal when aging the devices in air with RH 0%, N_2 with RH 95%, and N_2 with RH 0%. The aging tests were conducted at 120 °C. All sensing measurements were performed at room temperature in air with a N_2 carrier gas.

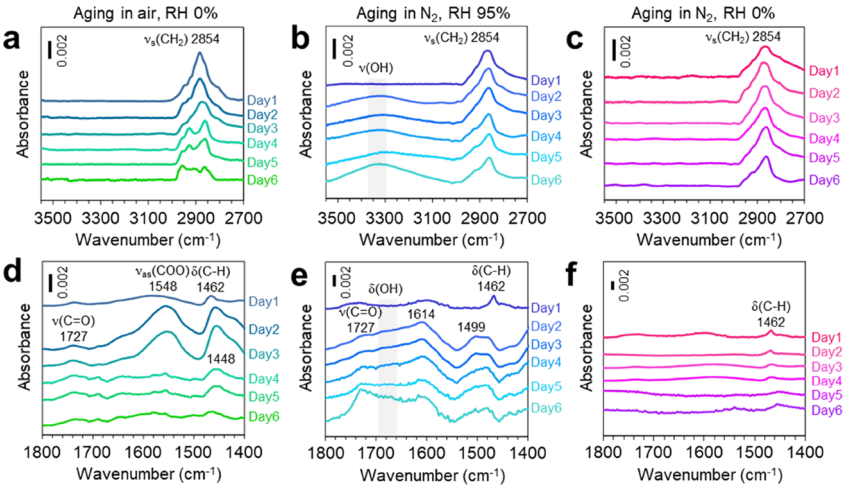

Figure 3. Time-dependent IR spectra of 2-way devices that were aged in (a,d) air with RH 0%, (b,e) N_2 with RH 95%, and (c,f) N_2 with RH 0%, respectively. Panels (a–c) show the regions for alkyl group (2800–3200 cm^{-1}) and hydroxyl group (3100–3500 cm^{-1}) and panels (d–f) show the carbonyl region (C═O and COO, 1400–1800 cm^{-1}). The aging tests were conducted at 120 °C.

in the PEG–CB nanocomposite sensor under an air environment (Figure 1e).

To obtain an in-depth understanding of the degradation mechanism of the PEG–CB nanocomposite sensor in terms of

https://doi.org/10.1021/acssensors.1c01875
ACS Sens. 2022, 7, 151–158

the chemical states, we next performed Fourier transform infrared (FTIR) spectroscopy measurements during the aging tests and compared the results with their molecular sensing data by using the 2-way device. Figure 3 shows the time-dependent FTIR spectra of the 2-way device during the aging tests in (a,d) air with RH 0%, (b,e) N_2 with RH 95%, and (c,f) N_2 with RH 0%, respectively. The aging tests were conducted at 120 °C. Figure 3a−c shows the regions for alkyl group (2800−3200 cm^{-1}) and hydroxyl group (3100−3500 cm^{-1}) and Figure 3d−f shows the carbonyl region (C═O and COO, 1400−1800 cm^{-1}). Similar to the sensing responses shown in Figure 2d, significant variations of IR spectra were observed after Day 2 in air with RH 0% (Figure 3d) and in N_2 with RH 95% (Figure 3b,e), while no obvious variation was seen in N_2 with RH 0% (Figure 3c,f). These trends well correspond to the degradation of the sensing responses shown in Figure 2d and also remind us of the crucial role of oxygen and water. Here, we first discuss the variation of the chemical state of the nanocomposite sensor induced by oxygen. For the aging test in air with RH 0%, three peaks tended to appear at around 1448, 1548, and 1727 cm^{-1} in the carbonyl region (Figure 3d), which are associated with the vibrations of carboxyl groups ν_s(COO) and ν_{as}(COO) and carbonyl group ν(C═O), respectively.[38] They correlate with the formation of aldehyde, formic acid, and acetic acid as oxidation products of PEG.[39−41] The peaks of ν_s(COO) and ν_{as}(COO) became smaller after Day 4, implying the removal of oxidation products. Such formation/removal of carboxyl groups might be irreversible phenomena because they involve the variation of alkyl group as shown in Figure 3a. A similar tendency was observed in the IR spectra of PEG (without CB) but not CB (Figure S5). These results clearly indicate that the oxidation of PEG triggered the degradation of the sensing response.

Next, we discuss how the chemical state of the PEG−CB nanocomposite sensor varies due to water. For the aging test in N_2 with RH 95%, several peaks tend to appear at around 1460−1540 cm^{-1}, 1580−1760 cm^{-1}, and 3100−3500 cm^{-1}. Two broad peaks at around 1650−1700 cm^{-1} and 3100−3500 cm^{-1} are assigned to δ(OH) and ν(OH), which plausibly originate from the adsorption of water molecules.[42] Consistent results were observed in the sensor resistance, that is, the sensor resistance decreased due to the ionic conduction of adsorbed water (Figure S4). The peak at 1727 cm^{-1} assigned to ν(C═O) tended to be larger during the aging test, which was plausibly due to the formation of an aldehyde group via the gradual oxidation of PEG in aqueous solution.[43] The other peaks at 1614 and 1499 cm^{-1} were almost unchanged after Day 2. These peaks were sometimes observed in a previous study of PEG while their origins are unclear.[44] Unlike the aging test in air with RH 0%, no significant variation in alkyl group was observed. These results imply that the basic structure of PEG was maintained during the aging test in N_2 with RH 95%. In order to investigate the effect of adsorbed water on the aging of PEG, we performed a thermal treatment to remove the adsorbed water molecules. Figure 4a shows the sensing responses of the 2-way device to 2.7 ppm nonanal at the initial state, after 5 days of aging in N_2 with RH 95% and after 48 h of annealing in N_2 with RH 0%, and Figure 4b,c shows the corresponding IR spectra. Remarkably, the degraded sensing response was recovered to 90% of its initial state after annealing. Consistent results were also observed in the IR spectra, that is, all peaks emerged during the aging test disappeared after the annealing and the shape of the IR spectrum changed back to the initial one. The results indicate that the adsorbed water does not cause fatal degradation in PEG and the

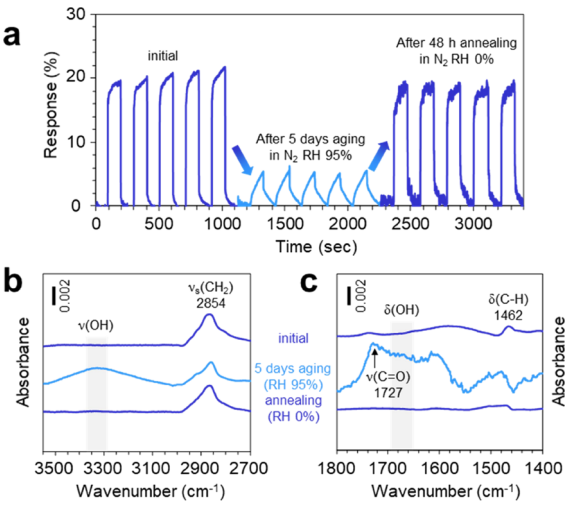

Figure 4. (a) Successive sensing responses of the 2-way device to 2.7 ppm nonanal at the initial state after 5 days of aging in N_2 with RH 95% and after 48 h of annealing in N_2 with RH 0% for dehydration, respectively. The aging test and thermal annealing were conducted at 120 °C. All sensing measurements were performed at room temperature in air with N_2 carrier gas. (b,c) IR spectra of the 2-way device at the initial state after 5 days of aging in N_2 with RH 95% and after 48 h of annealing in N_2 with RH 0% for dehydration, respectively. Panel (b) shows the regions for alkyl group (2800−3200 cm^{-1}) and hydroxyl group (3100−3500 cm^{-1}) and panel (c) show the carbonyl region (C═O and COO, 1400−1800 cm^{-1}).

sensing response. Also, they clearly highlight that the fatal degradation of the nanocomposite sensor is solely induced by the oxidation of PEG.

Here, we consider why the oxidation of PEG led to the degradation of the sensing response in the PEG−CB nanocomposite sensor. The comparison of molecular sensing data and IR spectra (Figures 2d and 3d) on the same device shows that the degradation of the sensing response was triggered by the oxidation of PEG and further progressed even when the oxidation products were removed. First, we consider that the chemical state of oxidized PEG caused the degradation of the sensing response. This is because the adsorption of analyte molecules and the resultant volumetric change in the polymer−carbon nanocomposite sensor are strongly determined by the affinity between analyte molecules and the polymer material. However, the observed sensor degradation might not be governed by the chemical state of oxidized PEG since a similar degradation trend in sensing response was seen when examining the molecular sensing using the higher polarity molecule of methanol (Figure S6). Next, we assume that the consumption of PEG seriously caused the degradation of the sensing response. This is because the total volumetric change of the nanocomposite sensor during molecular sensing must be suppressed when the amount of PEG is reduced. In fact, the sensing response tended to decrease with decreasing amount ratio of PEG in the PEG−CB nanocomposite (Figure S7). In principle, the oxidation of PEG involves cleavage of the C−C bond.[39−41] Therefore, PEG is supposed to be shorter and consumed via oxidation and the following removal of COO bonds as CO_2 gas (Figure 5a) as implicated by the IR spectra in Figure 3a,d. To directly validate the consumption of PEG, we evaluated the weight of PEG during the aging test in air. As we expected, the weight of PEG drastically decreased during the aging test in air with RH 0% (Figure 5b). Thus, we conclude that the

https://doi.org/10.1021/acssensors.1c01875
ACS Sens. 2022, 7, 151−158

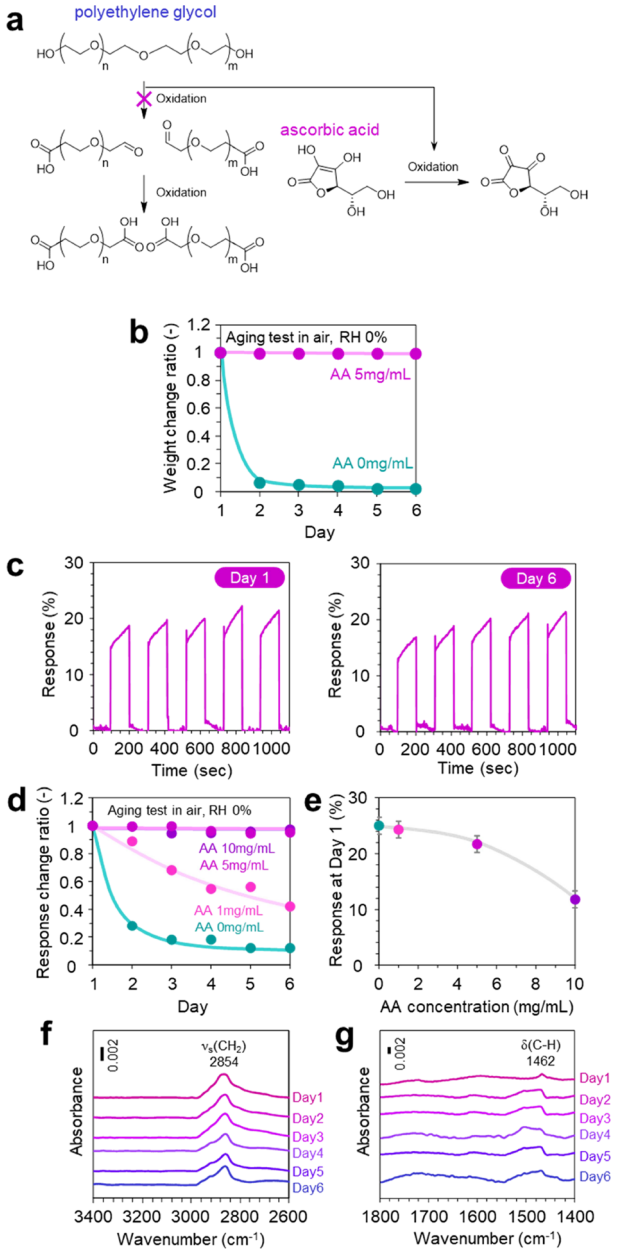

Figure 5. (a) Degradation mechanism of PEG and the proposed approach for suppressing degradation using AA. (b) Duration of weight (i.e., weight change ratio) of PEG and 5 mg/mL AA-added PEG during the aging test. (c) Successive sensing responses of the 5 mg/mL AA-added 2-way device to 2.7 ppm nonanal at Day 1 and Day 6 during the aging test. (d) Durations of the sensing response (i.e., response change ratio) to 2.7 ppm nonanal and (e) sensor resistance of the 2-way device with various AA concentrations. All sensing measurements and characterization of sensor resistance were performed at room temperature in air with N_2 carrier gas. (f,g) Time-dependent IR spectra of the 5 mg/mL AA-added 2-way device during the aging test. Panel (f) shows the regions for alkyl group (2800−3200 cm^{-1}) and hydroxyl group (3100−3500 cm^{-1}) and panel (g) shows the carbonyl region (C═O and COO, 1400−1800 cm^{-1}). The aging test was conducted at 120 °C in air at with RH 0%.

consumption of PEG, triggered by the oxidation, is responsible for the degradation of the sensing response.

The above results suggest that preventing the oxidation of PEG is of crucial importance to achieve the long-term stability of the PEG−CB nanocomposite sensor. In this regard, we examined the addition of an antioxidizing agent (i.e., ascorbic acid (AA))[43] to the nanocomposite sensor. We expect that the oxidation of PEG is prevented by alternatively oxidizing AA as schematically shown in Figure 5a. In fact, the consumption of PEG was drastically suppressed by the AA addition (Figure S8). Figure 5c shows the successive sensing response of the 2-way device to 2.7 ppm nonanal at Day 1 and Day 6 for the aging test in air with RH 0% when AA of 5 mg/mL was added to the nanocomposite. The aging test was conducted at 120 °C. Contrary to the result shown in Figure 2c, no significant degradation of the sensing response was seen in the AA-added nanocomposite sensor. The effect of the antioxidizing agent is more clearly seen in Figure 5d. The degradation of the sensing response can be prevented by increasing the AA concentration. Note that excess AA addition over 10 mg/mL resulted in the lowering of the sensing response (Figures 5e and S8). This implies that the excess AA interferes with the interaction between PEG and analyte molecules. The effect of AA addition on the suppression of degradation in the sensing response was also confirmed by acetone sensing, showing the diverse applicability of the present approach to various analytes (Figure S9). Figure 5f,g shows the IR spectra of the 2-way device during the aging test in air with RH 0% when AA of 5 mg/mL was added to the nanocomposite. The peaks associated with AA cannot be seen at the examined concentration condition (Figure S10). The appearance of ν_s (COO) and ν_{as} (COO) peaks and the variation of alkyl group were not seen in the spectra, indicating that the oxidation of PEG is substantially prevented by adding AA. Such a trend was well consistent with the results of the X-ray diffraction (XRD) measurement (Figure S11). Thus, these results indicate that the oxidation of PEG, which is responsible for the degradation of the PEG−CB nanocomposite sensor, was successfully prevented while maintaining the sensing response by adding an antioxidizing agent (i.e., AA) with a precisely controlled concentration.

Finally, we examined the long-term stability of a PEG−CB nanocomposite sensor. Figure 6a,b shows the optical microscopy images of an AA-added (5 mg/mL) PEG−CB nanocomposite sensor and its successive sensing response to 2.7 ppm nonanal at Day 1 and Day 30. For this experiment, the molecular sensing was performed once a day and the device was kept at room temperature in air with RH 67%. There are no significant variations in the morphology and the sensing response of the nanocomposite sensor. The effect of AA addition on the long-term stability of the nanocomposite sensor can be more clearly seen in Figure 6c. The degradation of the sensing response was significantly improved by adding AA while maintaining the amplitude of the sensing response. Also, the humidity-induced degradation of the sensing response was not seen. This is plausibly due to the fact that the adsorbed water in the nanocomposite sensor is removed by the self-Joule heating occurring during the molecular sensing measurement. Thus, the long-term stability of the PEG−CB nanocomposite sensor for 30 days was successfully achieved by rationally preventing the oxidation of PEG.

CONCLUSIONS

In conclusion, we conducted a mechanistic study for understanding the degradation of the sensing response and realizing long-term stability in a PEG−CB nanocomposite sensor under an air environment, which had been a bottleneck issue in polymer-based chemiresistive sensors. A device capable of performing both electrical molecular sensing and IR spectros-

https://doi.org/10.1021/acssensors.1c01875
ACS Sens. 2022, 7, 151−158

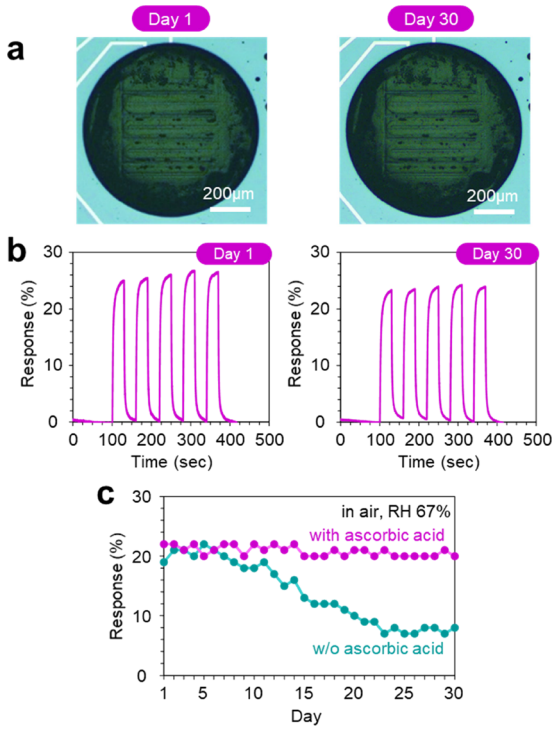

Figure 6. (a) Optical microscopy images of a PEG−CB nanocomposite sensor device with the addition of 5 mg/mL AA at Day 1 (left) and Day 30 (right). (b) Successive sensing responses to 2.7 ppm nonanal at Day 1 (left) and Day 30 (right). (c) Duration of the sensing response to 2.7 ppm nonanal with and without the addition of AA when storing the sensor sample at room temperature in air with RH 67%. All sensing measurements were performed at room temperature in air with N_2 carrier gas.

copy was designed to link the degradation of sensing response and the chemical state in a PEG−CB nanocomposite sensor. Comparison of the sensing properties and IR spectroscopy on the same device revealed that the oxidation-induced consumption of PEG is a crucial factor for the sensor degradation. According to the mechanism, we introduced an antioxidizing agent (i.e., AA) into the PEG−CB nanocomposite sensor to suppress the PEG oxidation and successfully demonstrated the long-term stability of sensing properties under an air environment for 30 days. Since oxidation is a common issue in polymer materials, the proposed approach is applicable to diverse polymer−carbon nanocomposite sensors for improving their long-term stability in an air environment.

EXPERIMENTAL SECTION

The polymer−CB nanocomposite used in this study was prepared by mixing CB (CB2350, Mitsubishi Chemical) and PEG (PEG4000, Aldrich Chemical Co.) in deionized water with the same quantity of 10 mg/mL. AA (Fujifilm Wako Pure Chemical Co.) was then added to the nanocomposite for suppressing the oxidation of PEG with a concentration of 0−10 mg/mL. The as-prepared nanocomposite was deposited on a Si substrate (n-type, capped with a 100 nm-thick SiO_2 layer) to fabricate two types of sensor devices including a component of 16-channel sensor array and an electrical sensing/IR spectroscopy 2-way sensor device. For the former sensor device, comb-shaped Pt electrodes with a Ti adhesive layer were first patterned on a 7×7 mm^2-sized substrate by combining photolithography and radio frequency sputtering. The gap distance and the thickness of Pt electrodes were 40 μm and 400 nm, respectively. A SU-8 photoresist layer with 45 μm thickness was then coated on the electrode-patterned substrate by spin-coating, and circular holes were patterned on the SU-8 layer by photolithography. The PEG−CB mixed solution was dropped on the patterned substrate by means of ink-jet printing (custom-made, SIJ Technology Inc.). For the latter device (i.e., electrical sensing/IR spectroscopy 2-way sensor device), Pt electrodes with a Ti adhesive layer were patterned on a 30×5 mm^2-sized substrate by means of metal mask. The gap distance and thickness of Pt electrodes for the 2-way device were 2 mm and 300 nm, respectively. The nanocomposite was then spin-coated on the electrode-patterned substrate with the condition of 2000 rpm for 200 s. Both sensor devices were then vacuum-annealed at 120 °C for 24 h to fully remove the solvent. The morphologies of the nanocomposite and the sensor device were characterized by field emission scanning electron microscopy (FESEM, JEOL JSM-7610F) at an accelerating voltage of 15 kV and optical microscopy (OLYMPUS DP21). XRD measurement was performed to evaluate the crystal structure of the nanocomposite. FTIR spectroscopy (Thermo Fisher Scientific Nicolet iS50) was performed for monitoring the degradation of the nanocomposite. The electrical properties and the molecular sensing response of the fabricated sensor devices were characterized by a probe station equipped with a gas supply system, a semiconductor parameter analyzer (Keithley 4200-SCS, for a 2-way device), and a homemade sensing module (for a component of the 16-channel sensor array). The molecular sensing measurements were conducted using 2.7 ppm nonanal, 5.6 ppm methanol, and 3.9 ppm acetone at room temperature in air. Nitrogen (N_2) was utilized as the carrier gas. The readout voltage was 1 V. The sensing response was defined as $(R_g - R_{N2})/R_{N2} \times 100\%$, where R_g and R_{N2} are the resistances of sensor devices exposed to nonanal and N_2, respectively. For the aging tests, the fabricated sensor devices were kept at 120 °C in air with RH 0%, N_2 with RH 95%, and N_2 with RH 0%. Five or six devices were fabricated and characterized for each aging condition in order to obtain reliable data.

ASSOCIATED CONTENT

Supporting Information

The Supporting Information is available free of charge at https://pubs.acs.org/doi/10.1021/acssensors.1c01875.

Surface morphology of the PEG−CB nanocomposite sensor; cycle dependence of successive nonanal sensing responses; nonanal sensing response with aging test in an oxygen atmosphere; variation of base resistance during aging tests; FTIR spectra for PEG4000 and CB with aging test; methanol sensing response with aging test; nonanal sensing response with varying CB/PEG ratios; nonanal sensing response with varying AA concentrations; acetone sensing response with aging test and AA addition; FTIR spectra of AA; XRD patters of the PEG−CB nanocomposite, PEG4000 and CB with aging test and AA addition; and morphological variation of the PEG−CB nanocomposite sensor with aging test and AA addition (PDF)

AUTHOR INFORMATION

Corresponding Authors

Kazuki Nagashima − *Department of Applied Chemistry, Graduate School of Engineering, The University of Tokyo, Tokyo 113-8656, Japan; PRESTO, Japan Science and Technology Agency, Kawaguchi-shi, Saitama 332-0012, Japan;* orcid.org/0000-0003-0180-816X; Email: kazu-n@g.ecc.u-tokyo.ac.jp

Takeshi Yanagida − *Department of Applied Chemistry, Graduate School of Engineering, The University of Tokyo, Tokyo 113-8656, Japan; Interdisciplinary Graduate School of Engineering Sciences, Kyushu University, Kasuga, Fukuoka 816-8580, Japan; Institute for Materials Chemistry and Engineering, Kyushu University, Fukuoka 816-8580, Japan;*

https://doi.org/10.1021/acssensors.1c01875
ACS Sens. 2022, 7, 151−158

orcid.org/0000-0003-4837-5701; Email: yanagida@g.ecc.u-tokyo.ac.jp

Authors

Wenjun Li − *Department of Applied Chemistry, Graduate School of Engineering, The University of Tokyo, Tokyo 113-8656, Japan; Interdisciplinary Graduate School of Engineering Sciences, Kyushu University, Kasuga, Fukuoka 816-8580, Japan*

Takuro Hosomi − *Department of Applied Chemistry, Graduate School of Engineering, The University of Tokyo, Tokyo 113-8656, Japan; PRESTO, Japan Science and Technology Agency, Kawaguchi-shi, Saitama 332-0012, Japan;* orcid.org/0000-0002-5649-6696

Chen Wang − *Interdisciplinary Graduate School of Engineering Sciences, Kyushu University, Kasuga, Fukuoka 816-8580, Japan*

Yosuke Hanai − *Panasonic Corporation, Industrial Solutions Company, Sensing Solutions Development Center, Kadoma, Osaka 571-8506, Japan*

Atsuo Nakao − *Panasonic Corporation, Industrial Solutions Company, Sensing Solutions Development Center, Kadoma, Osaka 571-8506, Japan*

Atsushi Shunori − *Panasonic Corporation, Industrial Solutions Company, Sensing Solutions Development Center, Kadoma, Osaka 571-8506, Japan*

Jiangyang Liu − *Department of Applied Chemistry, Graduate School of Engineering, The University of Tokyo, Tokyo 113-8656, Japan*

Guozhu Zhang − *Department of Applied Chemistry, Graduate School of Engineering, The University of Tokyo, Tokyo 113-8656, Japan*

Tsunaki Takahashi − *Department of Applied Chemistry, Graduate School of Engineering, The University of Tokyo, Tokyo 113-8656, Japan; PRESTO, Japan Science and Technology Agency, Kawaguchi-shi, Saitama 332-0012, Japan;* orcid.org/0000-0002-2840-8038

Wataru Tanaka − *Department of Applied Chemistry, Graduate School of Engineering, The University of Tokyo, Tokyo 113-8656, Japan*

Masaki Kanai − *Institute for Materials Chemistry and Engineering, Kyushu University, Fukuoka 816-8580, Japan*

Complete contact information is available at: https://pubs.acs.org/10.1021/acssensors.1c01875

Author Contributions

Sample preparation and characterization were performed by W.L., C.W., Y.H., A.N., and A.S. Fabrication and sensing measurements of chemiresistive sensor devices were conducted by W.L., C.W., Y.H., A.N., A.S., and J.L. FTIR measurements were performed by W.L. and C.W. The degradation mechanism of the polymer−CB nanocomposite chemiresistive sensor was discussed by W.L., K.N., T.H., Y.H., G.Z., T.T., W.T., M.K. and T.Y. K.N., Y.H., and T.Y. designed the experiments. K.N. wrote this manuscript and W.L., T.H., T.T., T.W., M.K., and T.Y. contributed to improve the manuscript. All authors contributed to the manuscript preparation and approved the final version of the manuscript.

Notes

The authors declare no competing financial interest.

ACKNOWLEDGMENTS

This work was supported by the Cooperative Research Program of "Network Joint Research Center for Materials and Devices," KAKENHI (Grant Numbers JP18H01831, JP18KK0112, JP18H05243, and JP20H02208) and CAS-JSPS Joint Research Projects (Grant No. JPJSBP120187207). K.N. and T.H. were supported by the MEXT Project of "Integrated Research Consortium on Chemical Sciences." T.Y. was supported by CREST (Grant No. JPMJCR19I2) and Mirai R&D of Japan Science and Technology Corporation (J.S.T.). K.N. was supported by JST PRESTO (Grant No. JPMJPR19J7). K.N. acknowledges the JACI Prize for Encouraging Young Researcher. This work was partly performed under the Cooperative Research Program of "Dynamic Alliance for Open Innovation Bridging Human, Environment, and Materials" and "CORE Lab of Network Joint Research Center for Materials and Devices."

REFERENCES

(1) Li, K.; Shao, Y.; Yan, H.; Lu, Z.; Griffith, K. J.; Yan, J.; Wang, G.; Fan, H.; Lu, J.; Huang, W.; Bao, B.; Liu, X.; Hou, C.; Zhang, Q.; Li, Y.; Yu, J.; Wang, H. Lattice-contraction triggered synchronous electrochromic actuator. *Nat. Commun.* **2018**, *9*, 1−11.

(2) Al-Turjman, F.; Lemayian, P. Intelligence, security, and vehicular sensor networks in internet of things (IoT)-enabled smart-cities: An overview. *Comput. Electr. Eng.* **2020**, *87*, No. 106776.

(3) Zhang, L.; Tian, F.; Nie, H.; Dang, L.; Li, G.; Ye, Q. Classification of multiple indoor air contaminants by an electronic nose and a hybrid support vector machine. *Sens. Actuators, B* **2012**, *174*, 114−125.

(4) Eusebio, L.; Derudi, M.; Capelli, L.; Nano, G.; Sironi, S. Assessment of the indoor odour impact in a naturally ventilated room. *Sensors* **2017**, *17*, 778.

(5) Macías, M. M.; Manso, A. G.; Orellana, C. J. G.; Velasco, H. M. G.; Caballero, G. R.; Chamizo, J. C. P. Acetic Acid Detection Threshold in Synthetic Wine Samples of a Portable Electronic Nose. *Sensors* **2013**, *13*, 208−220.

(6) Ampuero, S.; Bosset, J. O. The electronic nose applied to dairy products: a review. *Sens. Actuators, B* **2003**, *94*, 1−12.

(7) Ho, C. K.; Hughes, R. C. In-Situ Chemiresistor Sensor Package for Real-Time Detection of Volatile Organic Compounds in Soil and Groundwater. *Sensors* **2002**, *2*, 23−34.

(8) Wilson, A. D. Review of Electronic-nose Technologies and Algorithms to Detect Hazardous Chemicals in the Environment. *Procedia Technol.* **2012**, *1*, 453−463.

(9) Wang, B.; Cancilla, J. C.; Torrecilla, J. S.; Haick, H. Artificial Sensing Intelligence with Silicon Nanowires for Ultraselective Detection in the Gas Phase. *Nano Lett.* **2014**, *14*, 933−938.

(10) Nakhleh, M. K.; Amal, H.; Jeries, R.; Broza, Y. Y.; Aboud, M.; Gharra, A.; Ivgi, H.; Khatib, S.; Badarneh, S.; Har-Shai, L.; Glass-Marmor, L.; Lejbkowicz, I.; Miller, A.; Badarny, S.; Winer, R.; Finberg, J.; Cohen-Kaminsky, S.; Perros, F.; Montani, D.; Girerd, B.; Garcia, G.; Simonneau, G.; Nakhoul, F.; Baram, S.; Salim, R.; Hakim, M.; Gruber, M.; Gruber, M.; Ronen, O.; Marshak, T.; Doweck, I.; Nativ, O.; Bahouth, Z.; Shi, D.; Zhang, W.; Hua, Q.; Pan, Y.; Tao, L.; Liu, H.; Karban, A.; Koifman, E.; Rainis, T.; Skapars, R.; Sivins, A.; Ancans, G.; Liepniece-Karele, I.; Kikuste, I.; Lasina, I.; Tolmanis, I.; Johnson, D.; Millstone, S. Z.; Fulton, J.; Wells, J. W.; Wilf, L. H.; Humbert, M.; Leja, M.; Peled, N.; Haick, H. Diagnosis and Classification of 17 Diseases from 1404 Subjects via Pattern Analysis of Exhaled Molecules. *ACS Nano* **2017**, *11*, 112−125.

(11) Provost, F.; Fawcett, T. Data Science and its Relationship to Big Data and Data-Driven Decision Making. *Big Data* **2013**, *1*, 51−59.

(12) Bandodkar, A. J.; Jeerapan, I.; Wang, J. Wearable Chemical Sensors: Present Challenges and Future Prospects. *ACS Sens.* **2016**, *1*, 464−482.

(13) Lorwongtragool, P.; Sowade, E.; Watthanawisuth, N.; Baumann, R. R.; Kerdcharoen, T. A Novel Wearable Electronic Nose for

Healthcare Based on Flexible Printed Chemical Sensor Array. *Sensors* **2014**, *14*, 19700−19712.
(14) Chatterjee, S.; Castro, M.; Feller, J. F. An e-nose made of carbon nanotube-based quantum resistive sensors for the detection of eighteen polar/nonpolar VOC biomarkers of lung cancer. *J. Mater. Chem. B* **2013**, *1*, 4563−4575.
(15) Tomchenko, A. A.; Harmer, G. P.; Marquis, B. T.; Allen, J. W. Semiconducting metal oxide sensor array for the selective detection of combustion gases. *Sens. Actuators, B* **2003**, *93*, 126−134.
(16) Sun, Y. F.; Liu, S. B.; Meng, F. L.; Liu, J. Y.; Zhen, J.; Kong, L. T.; Liu, J. H. Metal Oxide Nanostructures and Their Gas Sensing Properties: A Review. *Sensors* **2012**, *12*, 2610−2631.
(17) Meng, G.; Zhuge, F. W.; Nagashima, K.; Nakao, A.; Kanai, M.; He, Y.; Boudot, M.; Takahashi, T.; Uchida, K.; Yanagida, T. Nanoscale Thermal Management of Single SnO_2 Nanowire: pico-Joule Energy Consumed Molecule Sensor. *ACS Sens.* **2016**, *1*, 997−1002.
(18) Wang, C.; Hosomi, T.; Nagashima, K.; Takahashi, T.; Zhang, G.; Kanai, M.; Yoshida, H.; Yanagida, T. Phosphonic Acid Modified ZnO Nanowire Sensors: Directing Reaction Pathway of Volatile Carbonyl Compounds. *ACS Appl. Mater. Interfaces* **2020**, *12*, 44265−44272.
(19) Liu, J.; Nagashima, K.; Nagamatsu, Y.; Hosomi, T.; Saito, H.; Wang, C.; Mizukami, W.; Zhang, G.; Samransuksamer, B.; Takahashi, T.; Kanai, M.; Yasui, T.; Baba, Y.; Yanagida, T. The impact of surface Cu^{2+} of ZnO/$(Cu_{1-x}Zn_x)$O heterostructured nanowires on the adsorption and chemical transformation of carbonyl compounds. *Chem. Sci.* **2021**, *12*, 5073−5081.
(20) Nekita, S.; Nagashima, K.; Zhang, G.; Wang, Q.; Kanai, M.; Takahashi, T.; Hosomi, T.; Nakamura, K.; Okuyama, T.; Yanagida, T. Face-Selective Crystal Growth of Hydrothermal Tungsten Oxide Nanowires for Sensing Volatile Molecules. *ACS Appl. Nano Mater.* **2020**, *3*, 10252−10260.
(21) Zhang, G.; Hosomi, T.; Mizukami, W.; Liu, J.; Nagashima, K.; Takahashi, T.; Kanai, M.; Sugiyama, T.; Yasui, T.; Aoki, T.; Baba, Y.; Ho, J. C.; Yanagida, T. *J. Mater. Chem.* **2021**, *9*, 5815−5824.
(22) Hu, N.; Karube, Y.; Arai, M.; Watanabe, T.; Yan, C.; Li, Y.; Liu, Y.; Fukunaga, H. Investigation on sensitivity of a polymer/carbon nanotube composite strain sensor. *Carbon* **2010**, *48*, 680−687.
(23) Ryan, M. A.; Shevade, A. V.; Zhou, H.; Homer, M. L. Polymer−carbon black composite sensors in an electronic nose for air-quality monitoring. *MRS Bull.* **2004**, *29*, 714−719.
(24) Zee, F.; Judy, J. W. Micromachined polymer-based chemical gas sensor array. *Sens. Actuators, B* **2001**, *72*, 120−128.
(25) Xie, H.; Yang, Q.; Sun, X.; Yang, J.; Huang, Y. Gas sensor arrays based on polymer-carbon black to detect organic vapors at low concentration. *Sens. Actuators, B* **2006**, *113*, 887−891.
(26) Chiou, J. C.; Wu, C. C.; Lin, T. M. Sensitivity Enhancement of Acetone Gas Sensor using Polyethylene Glycol/Multi-Walled Carbon Nanotubes Composite Sensing Film with Thermal Treatment. *Polymer* **2019**, *11*, 423.
(27) Wu, Z.; Chen, X.; Zhu, S.; Zhou, Z.; Yao, Y.; Quan, W.; Liu, B. Enhanced sensitivity of ammonia sensor using graphene/polyaniline nanocomposite. *Sens. Actuators, B* **2013**, *178*, 485−493.
(28) Wyszynski, B.; Yatabe, R.; Nakao, A.; Nakatani, M.; Oki, A.; Oka, H.; Toko, K. Array of Chemosensitive Resistors with Composites of Gas Chromatography (GC) Materials and Carbon Black for Detection and Recognition of VOCs: A Basic Study. *Sensors* **1606**, *2017*, 17.
(29) Yatabe, R.; Shunori, A.; Wyszynski, B.; Hanai, Y.; Nakao, A.; Nakatani, M.; Oki, A.; Oka, H.; Washio, T.; Toko, K. Odor Sensor System Using Chemosensitive Resistor Array and Machine Learning. *IEEE Sens. J.* **2021**, *21*, 2077−2083.
(30) Niu, L.; Luo, Y.; Li, Z. A highly selective chemical gas sensor based on functionalization of multi-walled carbon nanotubes with poly (ethylene glycol). *Sens. Actuators, B* **2007**, *126*, 361−367.
(31) Rahman, M. M.; Hussein, M. A.; Salam, M. A.; Asiri, A. M. Fabrication of an L-glutathione sensor based on PEG-conjugated functionalized CNT nanocomposites: a real sample analysis. *New J. Chem.* **2017**, *41*, 10761−10772.
(32) Kim, M.; Sowndhararajan, K.; Choi, H. J.; Park, S. J.; Kim, S. Olfactory Stimulation Effect of Aldehydes, Nonanal, and Decanal on the Human Electroencephalographic Activity, According to Nostril Variation. *Biomedicines* **2019**, *7*, 57.
(33) Syed, Z.; Leal, W. S. Acute olfactory response of Culex mosquitoes to a human-and bird-derived attractant. *Proc. Natl. Acad. Sci. U. S. A.* **2009**, *106*, 18803−18808.
(34) Ross, C. F.; Smith, D. M. Use of volatiles as indicators of lipid oxidation in muscle foods. *Compr. Rev. Food Sci. Food Saf.* **2006**, *5*, 18−25.
(35) Itoh, T.; Miwa, T.; Tsuruta, A.; Akamatsu, T.; Izu, N.; Shin, W.; Park, J.; Hida, T.; Eda, T.; Setoguchi, Y. Development of an exhaled breath monitoring system with semiconductive gas sensors, a gas condenser unit, and gas chromatograph columns. *Sensors* **2016**, *16*, 1891.
(36) Sakai, Y.; Matsuguchi, M.; Hurukawa, T. Humidity sensor using cross-linked poly(chloromethyl styrene). *Sens. Actuators, B* **2000**, *66*, 135−138.
(37) Gong, M. S.; Kim, J. U.; Kim, J. G. Preparation of water-durable humidity sensor by attachment of polyelectrolyte membrane to electrode substrate by photochemical crosslinking reaction. *Sens. Actuators, B* **2010**, *147*, 539.
(38) Wang, C.; Hosomi, T.; Nagashima, K.; Takahashi, T.; Zhang, G. Z.; Kanai, M.; Zeng, H.; Mizukami, W.; Shioya, N.; Shimoaka, T.; Tamaoka, T.; Yoshida, H.; Takeda, S.; Yasui, T.; Baba, Y.; Aoki, Y.; Terao, J.; Hasegawa, T.; Yanagida, T. Rational method of monitoring molecular transformations on metal-oxide nanowire surfaces. *Nano Lett.* **2019**, *19*, 2443−2449.
(39) Han, S.; Kim, C.; Kwon, D. Thermal/oxidative degradation and stabilization of polyethylene glycol. *Polymer* **1997**, *38*, 317−323.
(40) Hester, T. H.; Castillo, D. E.; Goebbert, D. J. Fragmentation of deprotonated polyethylene glycols, $[PEG - H]^-$. *Rapid Commun. Mass Spectrom.* **2013**, *27*, 1643−1648.
(41) Glastrup, J. Degradation of polyethylene glycol. A study of the reaction mechanism in a model molecule: tetraethylene glycol. *Polym. Degrad. Stab.* **1996**, *52*, 217−222.
(42) Nodari, L.; Ricciardi, P. Non-invasive identification of paint binders in illuminated manuscripts by ER-FTIR spectroscopy: a systematic study of the influence of different pigments on the binders' characteristic spectral features. *Herit. Sci.* **2019**, *7*, 1−13.
(43) Hemenway, J. N.; Carvalho, T. C.; Rao, V. M.; Venkatramana, M. R.; Yongmei, W.; Jaquan, K. L.; Ajit, S. N.; Srinivasa, R. P.; Howard, J. S.; Sailesh, A. V. Formation of reactive impurities in aqueous and neat polyethylene glycol 400 and effects of antioxidants and oxidation inducers. *J. Pharm. Sci.* **2012**, *101*, 3305−3318.
(44) Reddy, K. S.; Prabhakar, M. N.; Babu, P. K.; Venkatesulu, G.; Rao, U. S. K.; Rao, K. C.; Subha, M. C. S. Miscibility Studies of Hydroxypropyl Cellulose/Poly(Ethylene Glycol) in Dilute Solutions and Solid State. *Int. J. Carbohydr. Chem.* **2012**, *2012*, No. 906389.

https://doi.org/10.1021/acssensors.1c01875
ACS Sens. 2022, 7, 151−158